ONCOIMMUNOLOGY
2023, VOL. 12, NO. 1, 2150472
https://doi.org/10.1080/2162402X.2022.2150472

Taylor & Francis
Taylor & Francis Group

BRIEF REPORT

OPEN ACCESS Check for updates

Plasma galectins and metabolites in advanced head and neck carcinomas: evidence of distinct immune characteristics linked to hypopharyngeal tumors

Bao-Tram Thi Tran[a], Aurore Gelin[a], Sylvère Durand[b], Matthieu Texier[c], Amaury Daste[d], Clémence Toullec[e], Karim Benihoud[a], Ingrid Breuskin[f], Philippe Gorphe[f], Florence Garic[g], Catherine Brenner[a], Christophe Le Tourneau[h], Jérôme Fayette[i], Toshiro Niki[j], Muriel David[k], Pierre Busson[a*], and Caroline Even[f*]

[a]CNRS UMR 9018-METSY, Gustave Roussy and Université Paris-Saclay, Villejuif, France; [b]Plateforme de Métabolomique/UMR 1138, Gustave Roussy and Université Paris-Saclay, Villejuif, France; [c]Service d'Epidémiologie et de Biostatistiques, Gustave Roussy and Université Paris-Saclay, Villejuif, France; [d]Department of Medical Oncology, Hôpital Saint André, Bordeaux, France; [e]GI and Liver/Head and Neck unit, Institut du Cancer-Avignon Provence, Avignon, France; [f]Service de Cancérologie Cervico-Faciale, Gustave Roussy, Villejuif, France; [g]Department R&D, Unicancer, Paris cedex 13, France; [h]Department of Drug Development and Innovation (D3i), Institut Curie and Paris-Saclay University, Paris, France; [i]Claude Bernard Lyon 1 University, INSERM 1052, CNRS 5286 & Department of Medical Oncology, Centre Léon Bérard, Cancer Research Center of Lyon, Lyon, France; [j]Department of Immunology, Kagawa University, Kita-gun, Japan; [k]HiFiBiO Therapeutics, Pépinière Paris Santé Cochin, Paris, France

ABSTRACT

Extra-cellular galectins 1, 3 and 9 (gal-1, −3 and −9) are known to act as soluble immunosuppressive agents in various malignancies. Previous publications have suggested that their expression is dependent on the metabolic status of producing cells and reciprocally that they can influence metabolic pathways in their target cells. Very little is known about the status of gal-1, −3 and −9 in patients bearing head and neck squamous cell carcinomas (HNSCC) and about their relationships with the systemic metabolic condition. This study was conducted in plasma samples from a prospective cohort of 83 HNSCC patients with advanced disease. These samples were used to explore the distribution of gal-1, −3 and −9 and simultaneously to profile a series of 87 metabolites assessed by mass spectrometry. We identified galectin and metabolic patterns within five disease categories defined according to the primary site and human papillomavirus (HPV) status (HPV-positive and -negative oropharyngeal carcinomas, carcinomas of the oral cavity, hypopharynx and larynx carcinomas). Remarkably, samples related to hypopharyngeal carcinomas displayed the highest average concentration of gal-9 ($p = .017$) and a trend toward higher concentrations of kynurenine, a potential factor of tumor growth and immune suppression. In contrast, there was a tendency toward higher concentrations of fatty acids in samples related to oral cavity. These observations emphasize the diversity of HPV-negative HNSCCs. Depending on their primary site, they evolve into distinct types of immune and metabolic landscapes that seem to be congruent with specific oncogenic mechanisms.

ARTICLE HISTORY
Received 6 June 2022
Revised 16 November 2022
Accepted 17 November 2022

KEYWORDS
Head and neck carcinomas; plasma galectins; plasma metabolites; kynurenine

Introduction

Most malignant tumors of the upper aero-digestive tract are squamous cell carcinomas, often called head and neck squamous cell carcinomas (HNSCCs). They represent the sixth leading cause of cancer worldwide with an overall incidence of 650 000 new cases per year.[1,2] In most cases, the main etiological factors are alcohol and tobacco abuse. However, a fraction of them are related to infection by oncogenic viruses, notably human papillomavirus (HPV), mainly for two subtypes of oropharyngeal carcinomas: tonsil and basal tongue carcinomas.[3] The risk of distant metastases or locoregional recurrences is lower in HPV-positive carcinoma patients. Nevertheless, surgery and/or concomitant chemo-radiotherapy are still the standard of care for the treatment of non-metastatic primary HNSCCs regardless of their viral or non-viral etiology. Distant metastases and locoregional recurrences of HNSCCs remain a major therapeutic challenge requiring better treatments than conventional chemotherapy. For HNSCCs, like for other human malignancies, immunotherapy, especially immune checkpoint inhibitors (ICIs) targeting the PD1/PD-L1 axis, have improved patient outcomes. Immunotherapy can achieve durable responses for patients previously regarded as beyond therapeutic resources. However, only 20% of the patients with recurrent and/or metastatic disease benefit from immunotherapy, and it remains challenging to predict which patients will benefit from ICIs.[4–6]

The prevalence of alternative immune inhibitors is one mechanism suspected to explain primary or secondary resistance to ICIs in HNSCCs as well as in other human malignancies. Some of these alternative inhibitors are released in the extra-cellular medium and diffuse in the peripheral blood with potential systemic effects. This is the case, for example, for soluble Lag3 or HLA-G.[7,8] One category of alternative immune inhibitors often detected in the context of human malignancies are galectins, especially galectin-1, −3 and −9 (gal-1, −3 and −9).[9–11] In brief, galectins are lectins with selective affinity for

CONTACT Pierre Busson Pierre.BUSSON@gustaveroussy.fr CNRS UMR 9018-METSY, Gustave Roussy, 39, Rue Camile Desmoulins, F-94805 Villejuif, France
*Equal contributions

Supplemental data for this article can be accessed online at https://doi.org/10.1080/2162402X.2022.2150472

β-galactoside disaccharides that are contained in the carbohydrate moiety of glycoproteins and glycolipids. They are present in various intra-cellular compartments and involved in multiple cellular functions from RNA splicing to plasma membrane organization and surface receptor recycling.[12] Although they have no signal sequence, several galectins can be secreted in the extra-cellular space through non-conventional pathways like translocation through the plasma membrane or association with extra-cellular vesicles.[13] Galectins released by malignant or stromal cells can behave like cytokines having mainly immunosuppressive functions.[11,14,15] Regarding HNSCCs, there are clues suggesting that several extra-cellular galectins, especially gal-1, gal-3 and gal-9 play a role in tumor immune escape.[16–18] There are also data suggesting reciprocal interactions between galectin production and metabolic alterations occurring in the context of malignant diseases. For example, hypoxia has been shown to enhance gal-3 expression in malignant cells and/or tumor-associated macrophages (TAMs) in various types of malignancies.[19–21] Reciprocally, gal-3 facilitates the uptake of glucose, especially in endothelial cells, at least in part by up-regulation of the membrane transporter Glut-4.[22] In addition, high production of lactate enhances gal-9 expression in HNSCCs.[23] Therefore, this work intended to provide more information about the status of gal-1, −3 and −9 in HNSCCs in connection with their systemic metabolic status. We chose to profile gal-1, −3 and −9 and simultaneously a panel of metabolites in the peripheral blood of HNSCC patients more precisely in plasma samples. The primary reason for this approach is that galectins and other cancer-related metabolites are known to promote immune suppression not only in the tumor microenvironment but also at the systemic level, including in the peripheral blood. A second reason is that regarding biomolecules released by malignant cells or stromal cells, investigations on peripheral blood are a way to overcome the difficulties related to spatial tumor heterogeneity. The presence and concentration of these biomolecules in plasma samples are expected to reflect their status in various portions of the primary tumor or in multiple metastatic sites. Finally, in view of future longitudinal investigations, it is useful to rely on biological samples requiring only minimally invasive procedures.[24]

Practically, we assessed by ELISA the plasma concentrations of gal-1, −3 and −9, of C-reactive protein (CRP, a marker of inflammation) and CXCL9 chemokine (a marker of interferon-γ impregnation) in a prospective series of 83 patients with relapsed and/or metastatic HNSCCs. Simultaneously, we assessed by GC-MS the concentration of 87 metabolites detectable by our platform of metabolomics across most of our plasma samples with satisfactory quality controls. The whole work was done as an ancillary study of the TopNivo trial (NCT03226756). We found that the galectin and metabolite distributions were dependent on disease categories defined according to the primary tumor site and the HPV status. High concentrations of gal-9 and kynurenine (Kyn) were recorded in plasma samples related to hypopharyngeal carcinomas. In contrast, high concentrations of fatty acids were recorded in samples related to carcinomas of the oral cavity. This is a reminder that inside the vast group of HPV-negative HNSCCs, there are distinct types of tumor macroenvironments. High plasma levels of gal-9 appear to be characteristic of advanced hypopharyngeal carcinomas.

Materials and methods

Patients and healthy controls

TopNivo is a safety multicentric study of Nivolumab in patients with recurrent and/or metastatic platinum-refractory HNSCCs. Nivolumab injections were given every 2 weeks, up to 12 cycles (1 cycle = 28 days). A total of 351 patients have been enrolled in TopNivo (NCT03226756). In the last stage of the clinical trial recruitment, EDTA blood samples were obtained from 83 consecutive patients, at baseline, prior to the onset of Nivolumab. Plasma samples from anonymous healthy donors were used as controls. They were purchased from Zenbio (NC, USA) (ages comprised between 19 and 65). The HPV status of oropharyngeal carcinomas was determined according to p16 expression detected by immunohistochemistry.

Preparation of plasma samples

For each patient, 6–9 ml of blood were collected on EDTA tubes, and plasma was separated from cells by centrifugation at 1700 g for 15 min at 20°C in less than 3 h from the time of the blood collection. About 4 ml of plasma was recovered and stored at −80°C in 3 aliquots.

ELISA kits for galectin-1, −3 and −9

Plasma galectin-1 (gal-1), galectin-3 (gal-3) and galectin-9 (gal-9) concentrations were determined for all patients using the corresponding Quantikine ELISA kits from BioTechne/R&D system (reference DGal 10, 30 and 90) as recommended by the manufacturer. All samples were treated in duplicate. According to previous reports, normal median concentrations for these assays are close to 18, 6 and 7 ng/ml for gal-1, −3 and −9, respectively.[25–28]

Plasma CXCL9 and CRP assay

Plasma CXCL9 concentrations were determined using the Human CXCL9/MIG Quantikine ELISA Kit from Biotechne/R&D system (REF DCX900) as recommended by the manufacturer. All samples were treated in duplicate. CRP assays were made using an immunoturbidimetric assay (Atelicca CH C-Reactive Protein 2 kit) according to the manufacturer's instructions (Siemens Healthineers France).

Plasma metabolite profiling by Gas Chromatography/Mass Spectrometry using the MRM mode (Multiple Reaction Monitoring)

Pre-analytical procedure. For each patient, 50 µL of crude plasma was mixed with 500 µL of ice-cold extraction mixture (methanol/water, 9/1 spiked with a cocktail of internal standards) and centrifuged after 5 min of incubation (10 min at 15 000 g, 4°C). One hundred and fifty µL aliquots of supernatant were transferred to glass vials and evaporated to be used for

Gas Chromatography combined with Mass Spectrometry (GC-MS). Then, 50 µL of methoxyamine (20 mg/ml in pyridine) was added on dried extracts, which were stored at room temperature in the dark, overnight. The day after, 80 µL of N-Methyl-N-trimethylsilyl-trifluoroacetamide were added, and the final derivatization was made at 40°C during 30 minutes. Samples were then transferred into vials and directly injected into the GC-MS system.

Sample analysis. GC-MS/MS was performed with a 7890A gas chromatograph (Agilent Technologies, Waldbronn, Germany) coupled with a triple quadrupole 7000C (Agilent) equipped with a high sensitivity electronic impact source (EI) operating in positive mode. This method was inspired by developments reported previously.[29] The scan mode was the MRM for biological samples. Peak detection and integration of the analytes were performed using the Agilent Mass Hunter quantitative software (B.07.01).[30] All targeted treated data were merged and cleaned with a dedicated R package (version 4.0) (@Github/Kroemerlab/GRMeta).

Quality control policy. A daily qualification of the instrumentation was set up with automatic tune. These qualifications were completed with double injections of standard mixes, at the beginning and at the end of the run, in addition to blank samples to control the background impurities. Moreover, pools of tested samples were used to check the column before the analysis with the proper biological matrix. The same pool was re-injected during the batch to monitor and correct analytical bias occurring through the acquisition and post-acquisition treatment of the signal (m/z, retention time, and sensitivity drifts). For each analyte, the corrected peak area was considered to be proportional to its concentration.

Data interpretation. was made using the MetaboAnalyst software (https://www.metaboanalyst.ca).

Exploration of online transcriptional data related to HNSCCs

Online RNAseq data related to the TCGA Firehose Legacy cohort of HNSCCs were accessed through C-BioPortal (https://www.cbioportal.org/study/summary?id=hnsc_tcga). This cohort includes data resulting from bulk RNAseq made on primary tumors from 522 HNSCC patients. Our analysis was focused on transcripts encoding three proteins: gal-9, IDO1 and HIF1α. Data related to these three transcripts have been extracted and classified according to tumor categories similar to those used for plasma samples: a) HPV-positive oropharyngeal carcinomas (oro/HPV$^+$), b) HPV-negative oropharyngeal carcinomas (oro/HPV$^-$), c) carcinomas of the oral cavity, d) hypopharynx and e) larynx carcinomas. The HPV status was based on the detection of p16 by immunohistochemistry like for the patients of the TopNivo cohort. Because the HPV status was not determined for a fraction of oropharyngeal carcinomas, we had to deal with one additional category named "oro ND". Gene expression levels for each tumor sample were expressed using V2 RSEM values (RNA-seq by Expectation-Maximization). The data extracted from the C-Bioportal database and classified according to the six above-mentioned categories are presented in detail in **Supplementary Tables S7 and S8.**

Statistical analyses

Most statistical tests were done using the Prism-GraphPad software except for the interpretation of metabolomic profiles covered by the MetaboAnalyst software. Kruskal-Wallis and Dunn's multiple comparison tests were applied for comparisons of biomolecule concentrations in plasma samples related to distinct disease categories. The Spearman correlation test was used to assess correlations between distributions of various pairs of biomolecules. The same methods were used to explore online data from the C-BioPortal database.

Ethical issues

This study was conducted in accordance with the Declaration of Helsinki[31] (2013) and subsequent amendments, ICH Good Clinical Practice (GCP) Guidelines (CPMP/ICH/135/95) and the following European Directive: 2001/20/CE. The Independent Ethics Committee "CPP Ile de France VIII" reviewed and approved the study documents, including the initial protocol, all subsequent amendments as well as all information and documents provided to each patient included in this study. The initial protocol was given a favorable opinion on May 23th, 2017 (approval number: 2017–000424-10).

Results

Elevated concentrations of gal-9, −1 and −3 in plasma samples from HNSCC patients

Our initial investigations were focused on plasma gal-1, −3 and −9. The main clinical characteristics of the patients are

Table 1. Summary of patient characteristics.

Tumor/Disease categories(1)	Details on primary tumor sites	No of patients	Mean Age	M/F	No of recurrences w/o distant metastases	No of patients with distant metastases
HPV-positive oropharyngeal carcinomas	Tonsil Base of tongue Vallecula	8	64	7/1	1	7
HPV-negative oropharyngeal carcinomas	Tonsil Base of tongue Vallecula	35	63	22/13	17	18
Carcinomas of the oral cavity	Floor of mouth Buccal mucosa Oral tongue Hard palate Oral cavity (others)	14	61	10/4	9	5
Hypopharyngeal carcinomas		16	64	14/2	2	14
Laryngeal carcinomas		10	68	8/2	4	6

(1) Based on the primary tumor site and the HPV status

presented in detail in **Supplementary Table S1** and summarized in Table 1. Their recurrent or metastatic diseases were classified in five broad categories on the basis of the primary tumor location and its HPV status. We recorded patients with lesions derived from 8 HPV-positive and 35 HPV-negative oropharyngeal carcinomas, 14 carcinomas of the oral cavity, 16 hypopharyngeal and 10 laryngeal carcinomas. This distribution of tumor categories is somehow surprising by comparison with other series of HNSCCs, especially from North America.[1,32,33] The number of HPV-positive oropharyngeal carcinomas appears strikingly low (8/83), while the number of hypopharyngeal carcinomas is relatively high (16/83). This probably results at least in part from a selection bias. Indeed, our series gather patients with relapsed lesions and/or metastases, thus increasing the proportion of the most aggressive tumors, which might result in a bias in favor of hypopharyngeal and against HPV-positive oropharyngeal carcinomas. Another reason for this peculiar distribution might be the lower frequency of HPV-positive carcinomas among HNSCCs in France compared to North America.

Median values for gal-1, −3 and −9 concentrations in samples from healthy donors were compatible with previous reports (**Supplementary Table S2**).[25–28] As shown in Figure 1a and with more details in **Supplementary Tables S2, S3 and S4**, for a substantial number of HNSCC patients, plasma galectin concentrations were above the maximum values recorded in healthy donors. This was observed for gal-1 (58/83, 70%), gal-3 (50/83, 60%) and to a lesser extent for gal-9 (19/83, 23%). Overall, the differences in median values between healthy donors and HNSCC patients were significant for each galectin (Mann-Whitney: $p < .0001$, based on data presented in Supplementary Tables S2 and S3).

Higher concentrations of plasma gal-9 linked to hypopharyngeal carcinomas

Next, we investigated possible differences in plasma galectin concentrations according to the tumor category (based on the primary tumor site and its HPV status) and/or the number of metastatic sites. Regarding plasma gal-1 and −3, there was no evidence of correlations between their concentrations and these clinical characteristics, except a trend toward higher concentrations of gal-3 for HPV-positive oropharyngeal carcinomas (Figures 1b,c). In contrast, the median concentration of gal-9 was greater in patients with lesions derived from hypopharyngeal carcinomas by comparison with the four other tumor categories taken either as separate entities or as a unique group ($p = .018$) (Figures 1d,g). Consistently, plasma gal-9 was above the highest concentrations recorded in healthy controls for 9 of 16 hypopharyngeal carcinomas cases versus 10 of 67 samples for other HNSCCs ($p = .016$ – Fisher's exact test) (**Supplementary Table S4**). Plasma gal-9 concentrations were also greater in patients with two or more metastatic sites compared to patients free of metastatic lesions ($p = .028$) (Figure 2c). In contrast, there was no significant difference between patients with a single metastasis and patients free of any metastatic lesion (Figure 2c). Because hypopharyngeal carcinomas are known to be more aggressive than other HNSCCs, we wanted to determine whether the high levels of plasma gal-9 recorded for this disease category were independent of their metastatic status.[32] Therefore, we resorted to multivariate analysis. Analysis by factorial Anova showed a significant effect of the primary tumor category even among patients with multiple metastatic sites ($p = .014$). Looking at the whole cohort, we found no link between plasma gal-9 concentration and the progression-free survival (**Supplementary Fig S1**).

Lack of correlations between galectin concentrations and levels of CRP and CXCL9 in plasma samples from HNSCC patients

It is well known that various cell types enhance their production of gal-1, gal-3 or gal-9 when they are in the context of nonspecific inflammation or high impregnation by γ-interferon.[34–36] Such conditions are common in the microenvironment and macroenvironment of HNSCCs.[1,33,37] Therefore, we used plasma CRP (C-reactive protein) as a marker of systemic inflammation and CXCL9 as a marker of impregnation by γ-interferon. Indeed, it is well known that plasma levels of CXCL9 often reflect the overall tissue production and activity of γ-interferon better than its own plasma concentration.[38] As shown in the **Supplementary Fig S2**, the correlations of galectin concentrations with CRP and CXCL9 concentrations were weak (r coefficients below 0.4 in the best cases). This suggests that systemic inflammation or excessive production of γ-interferon are not the main determinants for the elevated concentrations of plasma galectins in HNSCCs and that additional mechanisms are at play.

High levels of plasma kynurenine (Kyn) linked to high concentrations of plasma gal-9 and to hypopharyngeal carcinomas

As mentioned earlier, several previous studies have highlighted reciprocal influences of metabolic regulations, on the one hand, and gal-1, −3 and −9 expression and activity, on the other hand.[19–23] Therefore, we investigated whether some plasmatic metabolites were preferentially associated with high concentrations of gal-1, −3 and −9 and/or with a specific tumor category. To do so we applied a method of targeted mass spectrometry called MRM (Multiple Reaction Monitoring) characterized by concomitant scanning of multiple mass windows. It was operated with an inclusion list of 130 metabolites including metabolites of the tricarboxylic acid cycle, amino-acids and related molecules, fatty acids, eicosanoids and molecules related to plant-derived nutrients. The same plasma samples used for galectin assays were subjected to this procedure. After preliminary runs, 87 out of 130 metabolites were selected for subsequent analyses, based on their detection in the vast majority of plasma samples with satisfactory quality control (**list in Supplementary Table S5**). A correlation map including the 87 metabolites and the 5 proteins (gal-1, −3, −9, CRP and CXCL9) was built using the MetaboAnalyst software (Figure 3). Five main clusters were delimited on this map according to the boundaries of color contrasts and, to a lesser extent, the arborescence of the dendrogram. They were designated a, b, c, d, and e (details on their content are provided in

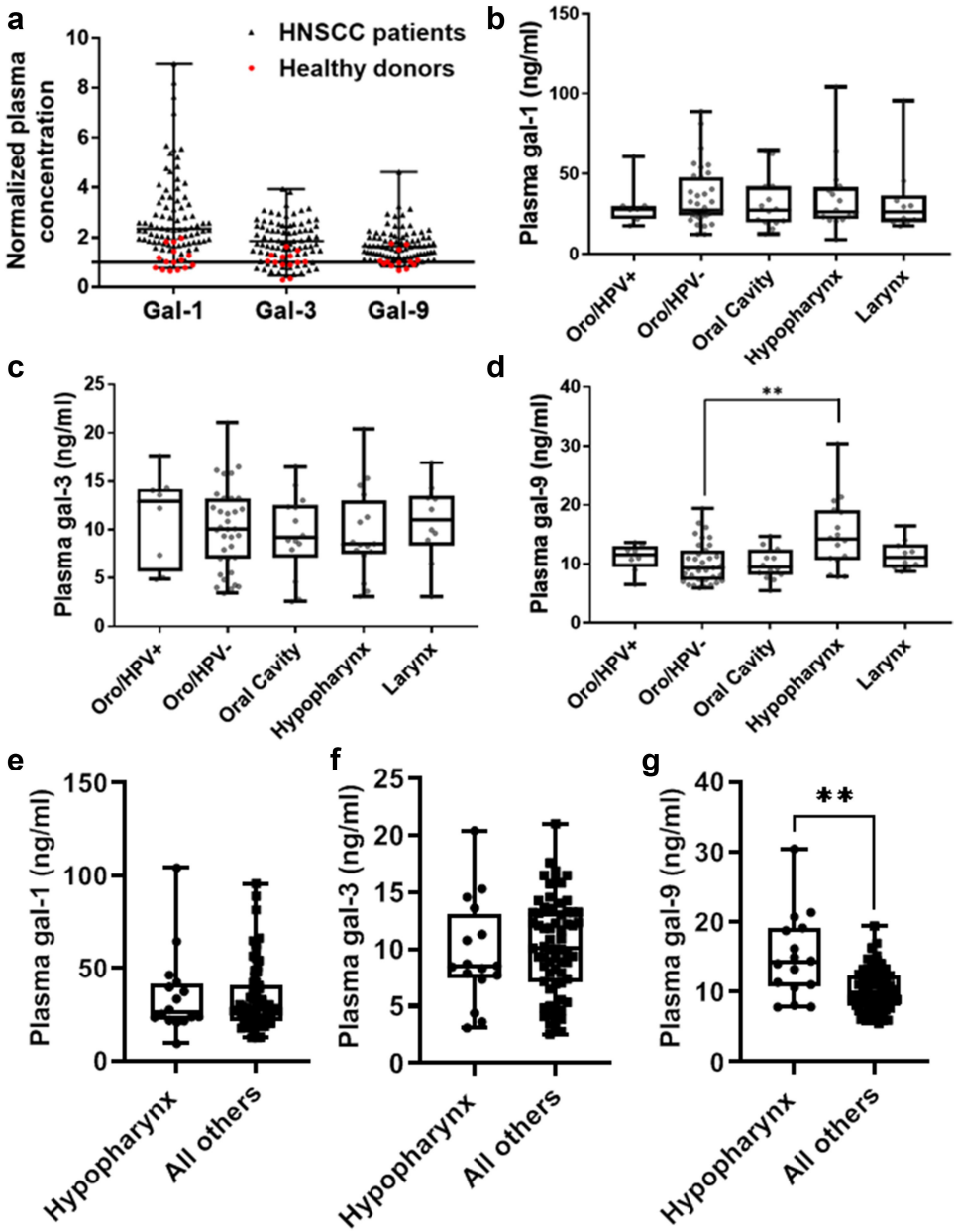

Figure 1. Overall distribution and distribution by tumor categories of gal-1, −3 and −9 concentrations in plasma samples from 83 HNSCC patients. A Overall distribution in all samples of the cohort and comparison with healthy donors. Plasma concentrations of galectins were determined by ELISA as explained in the Materials and Methods section. Values obtained for patients and healthy donors are shown as black and red dots, respectively. For gal-1, we had 15 measurements made in samples from 5 donors (lowest and highest concentrations 7.44 and 22.81 ng/ml, respectively; median: 11.64 ng/ml). For gal-3, we had 13 measurements made in samples from 5 donors (lowest and highest concentrations 1.51 and 8.70 ng/ml, respectively; median: 5.33 ng/ml). For gal-9, we had 13 measurements in samples from 4 donors (lowest and highest concentrations 4.28 and 13.39 ng/ml, respectively; median 6.57 ng/ml). For both patients and healthy donors, concentrations were normalized on the median concentration of the healthy donors. Fifty eight out of 83 patients, 50/83 and 19/83 patients had plasma concentrations above the highest value recorded in healthy donors for gal-1, gal-3 and gal-9 respectively. **b, c and d** Comparison of plasma galectin concentrations for five tumor categories: oropharyngeal (oro) HPV-pos and neg, oral cavity, hypopharynx, larynx. Kruskal-Wallis tests: gal-1: $p = .88$; gal-3: $p = .79$; gal-9: $p = .018$. For gal-9, all possible pairwise comparisons were tested using the Dunn's multiple comparisons test. The only significant difference regarding the distribution of plasma gal-9 concentrations was between hypopharynx and HPV-neg oropharynx carcinomas (**$p = .012$). **e, f and g** Comparison of plasma galectin concentrations recorded for hypopharyngeal carcinomas versus the four other categories taken as a single group. In accordance with data presented in B, C and D, the difference is statistically significant only for gal-9 (Mann–Whitney test: gal-1: $p = .93$; gal-3: $p = .46$; gal-9: $p = .0020$).

the legend of Figure 3). Briefly, the two largest clusters, a and b, mainly consisted of free proteinogenic amino-acids. Clusters c and e contained various types of biomolecules. Several fatty acids were found in cluster d (oleic, linoleic, and palmitoleic acids) and the related 3-hydroxybutyric acid. Gal-1, gal-3, CRP and CXCL9 were not included in any of these five clusters. In contrast, Gal-9 was included in cluster e. Additional information was provided by the supervised heat map showing relative plasma concentrations of the 87 metabolites and 5 proteins in connection with the tumor categories (Figure 4). According to the overall ANOVA statistical test, none of the metabolites showed significant differences in their distribution among distinct tumor categories. However, several metabolites close to gal-9 inside cluster e of the correlation map appeared

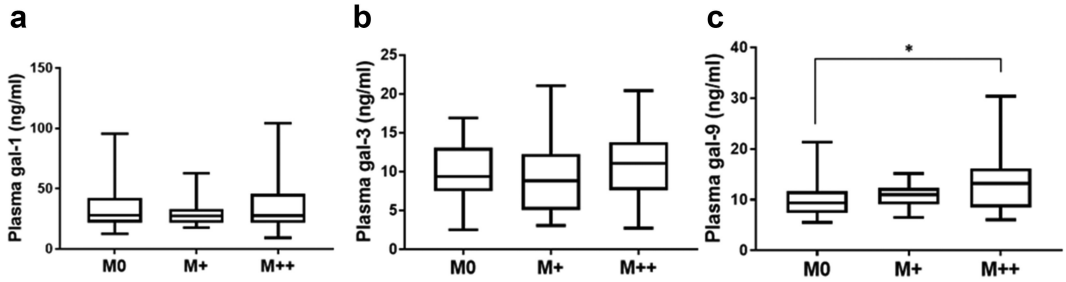

Figure 2. Distribution of plasma galectin concentrations according to the number of metastatic sites. M0: absence of any detectable metastatic site (n = 33); M+: only one metastatic site (n = 20); M++: two or more metastatic sites (n = 30). **a** Gal-1 (Kruskal–Wallis test: $p = .85$). **b** Gal-3 (Kruskal–Wallis test: $p = .45$). **c** Gal-9 (Kruskal–Wallis test: $p = .028$); all possible pairwise comparisons were tested using the Dunn's multiple comparisons test; the only significant difference regarding the distribution of plasma gal-9 was between M++ vs M0 patients (*$p = .022$). In contrast, the difference was not significant when comparing M+ and M0 patients ($p = .69$).

to be more abundant in samples from hypopharyngeal and laryngeal carcinomas than from other tumor categories (Figure 4). This was the case, for example, for Kyn, arabinol, erythritol and threonic acids. In contrast, three elements of cluster d, linoleic, palmitoleic and 3-hydroxybutyric acids were more abundant in samples from carcinomas of the oral cavity.

The distribution of plasma Kyn was analyzed with more details (Figure 5). As shown in Figure 5a there was a trend toward a higher concentration in samples related to hypopharyngeal and laryngeal carcinomas. Kyn is the main catabolite of tryptophan (Trp). As expected, an opposite trend was noted for the Trp/Kyn ratio, which was smaller for hypopharyngeal and laryngeal carcinomas than for other HNSCCs (Figure 5b). Kyn was significantly more abundant in plasma samples from patients with two metastatic sites than in the absence of metastases (Figure 5c). Finally, there was an overall correlation between gal-9 and Kyn concentrations among all HNSCCs (r CLOSE to 0.60) (Figure 5d). Interestingly, this correlation was even greater among hypopharyngeal carcinomas (r close to 0.77), while it was absent among laryngeal carcinomas (Figures 5e,f).

Correlation between gal-9 and IDO1 mRNAs detected in HNSCC primary tumors (transcriptional data from TCGA)

One obvious question was whether differences in plasma gal-9 and Kyn concentrations reflected the abundance of gal-9 and IDO1 proteins inside the tumor lesions (as previously mentioned, IDO1 is the main enzyme involved in the production of Kyn). For practical reasons, it was not possible to investigate the expression of these proteins either in the contemporary metastatic or recurrent lesions or in the corresponding primary tumors. Therefore, to get some possible clues about gal-9 and IDO1 expressions in various categories of HNSCCs, we mined online data resulting from bulk RNAseq in a TCGA cohort of HNSCCs (Firehose Legacy cohort).

As shown in Figure 6, we could observe some trends in the distribution of gal-9 and IDO1 transcripts in the various categories of HNSCCs. Their highest abundances were recorded in the category of HPV^+ oropharyngeal tumors (oro/HPV^+) with statistically significant differences when compared with oral cavity and larynx carcinomas. The median amounts of gal-9 and IDO1 mRNAs for hypopharyngeal carcinomas were in the lower range. HIF1α mRNA was also analyzed with two ideas in mind: 1) a possible link between tumor hypoxia and galectin expression (as mentioned in the introduction); 2) the frequent induction of HIF1α transcription in malignant cells undergoing hypoxia.[39] The distribution of HIF1α expression levels through the various categories of HNSCCs was quite different from those of gal-9 and IDO1. The highest abundance of HIF1α transcripts were recorded for HPV^- oropharyngeal carcinomas (oro/HPV^-).

Finally, when looking at the HNSCC cohort as a whole, a positive correlation was found between the tumor amounts of gal-9 and IDO1 mRNAs (Spearman coefficient r = 0.61, p < .0001). In contrast, there was a negative correlation between gal-9 and HIF1α as well as between IDO1 and HIF1α transcripts (Figure 6).

Discussion

Our exploratory study on the distribution of galectins and metabolites in the plasma from patients bearing advanced HNSCCs has several original characteristics. First, it deals with the tumor macroenvironment, in other words with the systemic aspects of the disease in contrast with almost all previous studies focused on the microenvironment of tumor lesions. Next, we have investigated the status of three galectins simultaneously in the same series of patients, in contrast with almost all previous studies focusing on one galectin in a given series. Finally, we have combined the exploration of the galectin status with GC-MS profiling of 87 metabolites.

Our main results can be summarized as follows: First, we show that gal-1, −3 and −9 are detected in the plasma of a fraction of HNSCC patients at a higher concentration than in healthy donors. This applied to more than 50% of the patients for gal-1 and gal-3 and to about 25% of the patients for gal-9. Regarding gal-1 and gal-3, our data are consistent with previous publications reporting high concentrations of gal-1 and gal-3 in a fraction of HNSCC serum samples.[18] We found no significant differences in the distribution of gal-1 and gal-3 concentrations according to the tumor category, despite a trend toward higher concentrations in HPV-positive oropharyngeal carcinomas. This observation is consistent with a recent publication reporting a greater abundance of gal-3 detected by immunohistochemistry in tumor sections from HPV-positive compared to HPV–negative HNSCCs.[40] Regarding gal-9, we found significantly higher concentrations

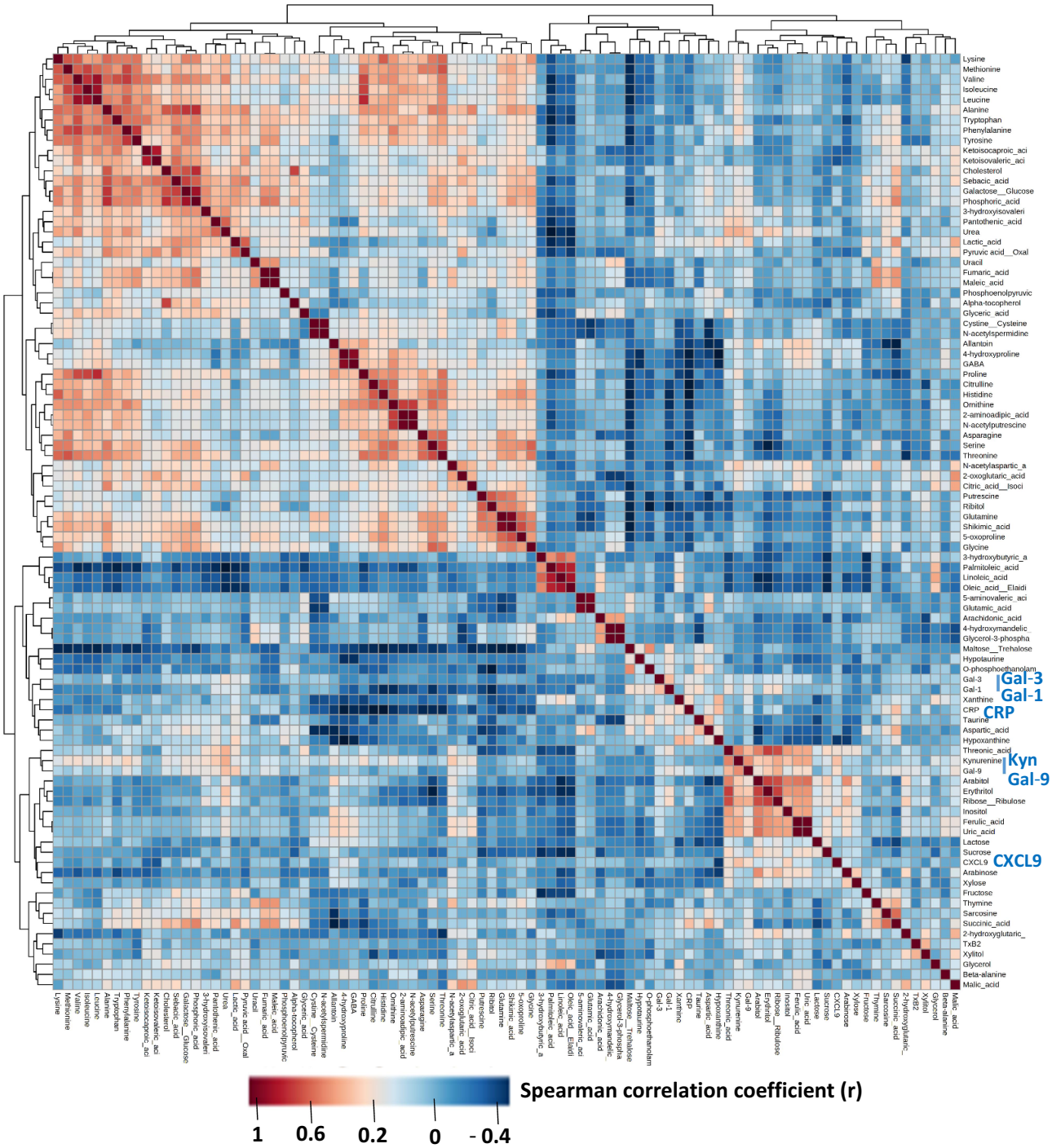

Figure 3. Overview and correlation mapping of the distribution of 87 metabolites detected by GC-MS and five selected proteins (gal-1, –3 and –9, CRP, CXCL9) in plasma samples from HNSCC patients. The correlation matrix was generated using the "correlation" function of the MetaboAnalyst software (https://www.metaboanalyst.ca). Data related to metabolites and proteins were analyzed simultaneously using the same software although they were obtained using distinct assays, GC/MS and ELISA respectively. The color scale is a function of Spearman coefficients of correlation. Areas of red colors signal biomolecules occurring with concomitant high abundance in substantial numbers of plasma samples. Five prominent clusters designated a, b, c, d, e were delimited on the basis of color contrasts and to a lesser extent dendrogram arborescence. Clusters a and b mainly consisted of free proteinogenic amino-acids including branched (valine, leucine, isoleucine) and aromatic (tryptophan, phenylalanine, tyrosine) amino-acids, proline, asparagine, serine and threonine as well as two non-proteinogenic amino-acids (citrulline and ornithine). Cluster c was heterogeneous including a polyamine, putrescine, glutamine and shikimic acid, a metabolite derived from plants and microorganisms. Cluster d consisted of 3 fatty acids (oleic, linoleic, palmitoleic acids) and the related 3-hydroxybutyric acid. Like cluster c, cluster e was heterogenous containing gal-9, kynurenine (Kyn), uric acid and 4 putative plant-derived metabolites (threonic and ferulic acids, arbitol and erythritol). While gal-9 was clearly linked to cluster e, just adjacent to Kyn, gal-1, gal-3, CRP and CXCL9 were not associated to well delimited clusters.

in plasma samples connected to the hypopharyngeal primary site, a correlation that was independent of the number of metastatic sites. We found no significant correlation between the galectin concentrations and concentrations of the CRP and CXCL9. Regarding the metabolic profiles, our most exciting observations were the high concentrations of Kyn in samples from hypopharyngeal carcinomas; not only Kyn was abundant in this category but there was a strong correlation with gal-9

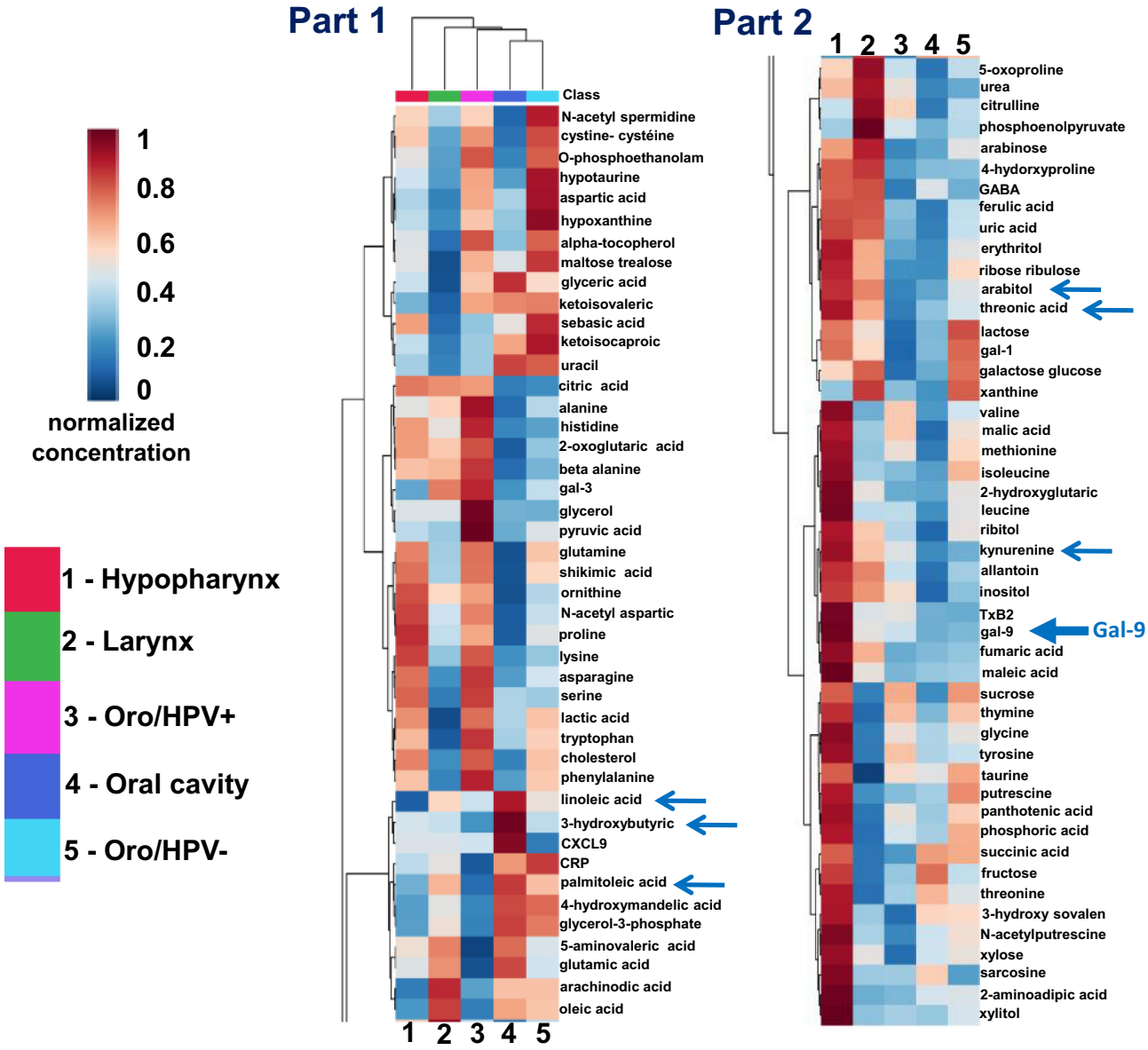

Figure 4. Supervised heatmap showing relative concentrations of metabolites and selected proteins in connection with tumor/disease categories. This heatmap was generated using the "heatmap" function of the MetaboAnalyst software. The color scale is a function of the relative concentration of each biomolecule (m/z peak areas for metabolites and pg/ml or ng/ml for proteins). It was assessed according to the positive or negative distance from the mean concentration recorded for each analyte in the 83 sample series. For better view and reading, the heatmap was split in two parts. "Oro" stands for oropharyngeal carcinomas. Overall, according to Anova statistical analysis, none of the metabolites on this map showed a significant difference of distribution between the 5 disease categories. However, it is noteworthy that a large number of metabolites (38/87) were at higher relative concentrations in plasma samples related to hypopharyngeal carcinomas. Most components of cluster E identified in Figure 4, especially one protein (gal-9; bold blue arrow) and several metabolites (kynurenine, arabitol, threonic acid; thin blue arrows, part 2)) were abundant in samples from hypopharyngeal carcinomas. In contrast, three components of cluster D (Figure 4) – linoleic, palmitoleic and 3-hydroxybutyric acid (thin blue arrows; part 1) – were abundant in samples from carcinomas of the oral cavity.

concentration, which was not the case for laryngeal carcinomas. Regarding carcinomas of the oral cavity, there was a trend toward higher concentrations of linoleic, palmitoleic and 3–hydroxybutyric acids.

Kyn is a metabolite related to amino-acids with important signaling capabilities. It results from the oxidation of tryptophan, one essential amino-acid which combines an indol heterocycle with a short lateral chain. Three dioxygenases can open the indol ring and produce Kyn: IDO1 (indoleamine 2, 3-dioxygenase 1), TDO (tryptophan 2,3-dioxygenase) and IDO2. These enzymes are expressed in various cell-types and tissues. IDO2 is present in the liver, which is not the case for IDO1. Their expression is enhanced by interferon-γ and lipopolysaccharide. TDO is present mainly in the liver, placenta and brain and is up-regulated by glucocorticoids.[41] All three enzymes are often expressed in malignant cells. Downstream of Kyn, there is the Kyn catabolic pathway that ultimately leads to the production of nicotinamide adenine dinucleotide (NAD^+) involving enzymes like kynureninase and kynurenine 3--monooxygenase.[42] Kyn is involved in immunosuppression. Initially, several studies had pointed to tryptophan starvation, rather than the direct effect of Kyn, as a major mechanism of T-cell inactivation. According to some ancient studies, the rise of Kyn production was mainly a side-effect concomitant of

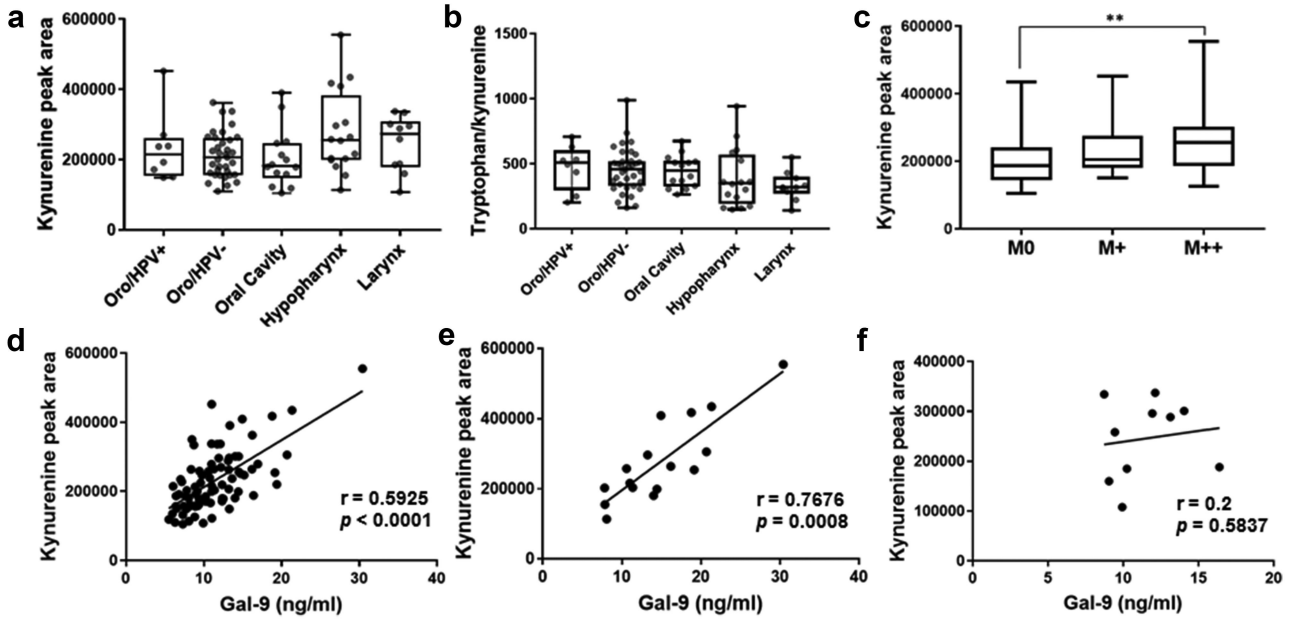

Figure 5. Variations of plasma kynurenine (Kyn) concentrations in connection with some clinical and biological characteristics of HNSCCs. a Comparison of the plasma Kyn concentrations according to the five tumor categories: oropharyngeal (oro) HPV-pos and neg, oral cavity, hypopharynx, larynx. Kyn concentrations were estimated from the areas under the corresponding m/z peak curves corrected according to quality control data. There was a trend toward higher concentrations for plasma samples related to hypopharyngeal and laryngeal carcinomas (Kruskal-Wallis $p = .18$). **b** Comparisons of the ratios of Tryptophan/Kyn concentrations in the five tumor categories. **c** Distribution of plasma Kyn concentrations according to the number of metastatic sites; M0: absence of any detectable metastatic site (n = 33); M+: only one metastatic site (n = 20); M++: two or more metastatic sites (n = 30) (Kruskal–Wallis test: $p = .016$ – Dunn's multiple comparisons test: M++ vs M0 $p = .015$); **d** Correlations of gal-9 concentrations (based on ELISA) with Kyn concentrations (based on mass spectrometry) for plasma samples of the whole HNSCC cohort (83 patients)(Spearman test). **e and f** Same correlations restricted to plasma samples related to hypopharyngeal (e) and laryngeal (f) carcinomas.

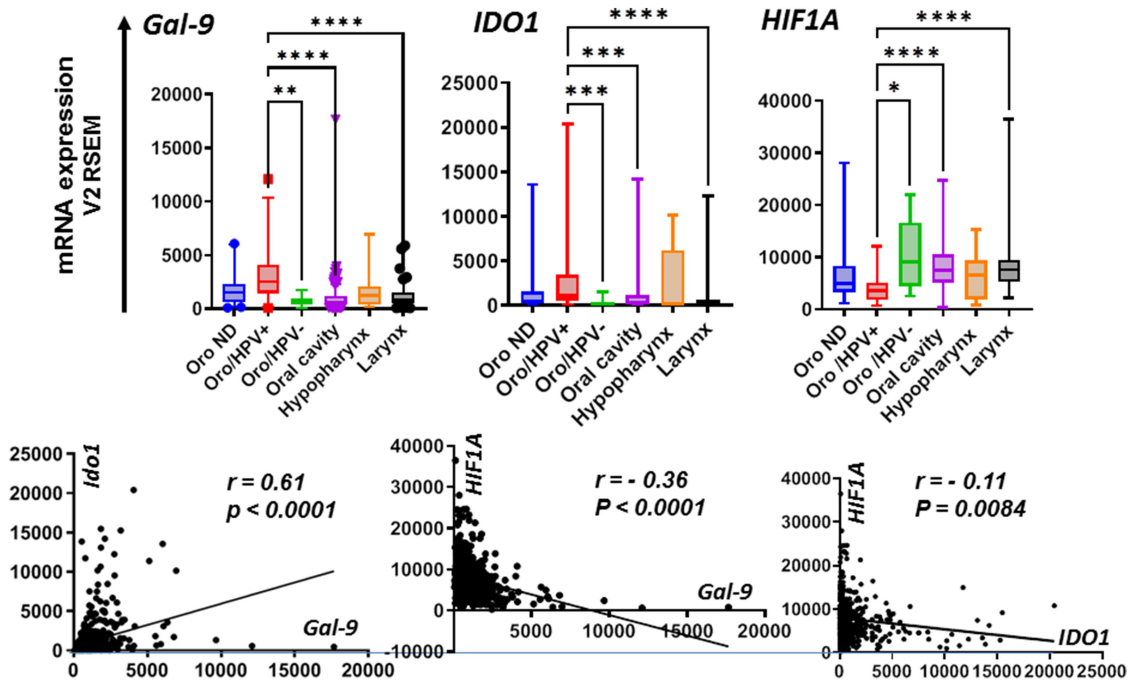

Figure 6. Status of gal-9, IDO1 and HIF1α transcripts in the various categories of HNSCCs according to TCGA online data (access through C-BioPortal – Firehose Legacy cohort). Oro ND: oropharyngeal carcinomas with unknown HPV status (n = 39); oro/HPV^{+}: HPV-positive oropharyngeal carcinomas (n = 33); oro/HPV^{-}: HPV-negative oropharyngeal carcinomas (n = 8); carcinomas of the oral cavity (n = 316); hypopharynx (n = 10) and larynx (n = 116). Total number of cases: 522. **Upper panel**: there are significant differences in the distribution of the Gal-9, IDO1 and HIF1α transcripts through the various categories of HNSCCs (Kruskal–Wallis test: $p = .001$)(error bars: standard error of the mean). Pairwise comparisons have been made using Dunn's tests. Brackets and asterisks are shown only for significant comparisons involving oro/HPV^{+} (* p < .05; ** p < .01; *** p < .001; **** p < .0001). We found no significant comparisons involving hypopharyngeal carcinomas. **Lower panel**: correlations between the amounts of gal-9, IDO1 and HIF1α transcripts in the overall cohort of HNSCCs given using V2 RSEM values (RNA-seq by Expectation-Maximization). A positive correlation is found between the tumor amounts of gal-9 and IDO1 mRNAs. In contrast, there is a negative correlation between HIF1α and Gal-9 as well as HIF1α and IDO1 transcripts.

tryptophan catabolism. However, more recent studies have challenged this interpretation, especially since Kyn was identified as a ligand of the aryl hydrocarbon receptor (AhR), a ligand-activated transcription factor. Stimulation of AhR inside T-cells is known to favor the onset of immunosuppressive phenotypes, especially their differentiation into T-regs.[43] In addition, it stimulates the cooperation of T-regs with tumor associated macrophages (TAMs) having M2 polarity.[44] Moreover, Kyn has been reported to have direct oncogenic effects, for example by activating β-catenin signaling in mouse colon cancer models.[45] It can also induce a switch from programmed cell death to a program of tumor cell dormancy. This effect is dependent on AhR.[41] Therefore, Kyn can be regarded as a candidate onco- and immune-metabolite.

It is interesting to note that the concentration of plasma gal-9 and, possibly, of plasma Kyn are consistently higher in samples related to hypopharyngeal carcinomas in comparison with other HNSCCs. One important lesson from this observation is that there is biological heterogeneity among HPV-negative HNSCCs. In the medico-scientific literature, there is a strong and somehow surprising tendency to oppose only two major subsets of HNSCCs either HPV-positive or HPV-negative.[33,46] However, one should keep in mind the dissymmetry of these two categories. Most HPV-positive HNSCCs arise from the epithelium of the tonsils or from the base of the tongue.[3] On the other hand, the anatomic origins of HPV-negative HNSCCs are much more diverse, including multiple sites in the rest of the oropharynx, in the oral cavity, larynx and hypopharynx. Despite the similarity of some risk factors and oncogenic events, the diversity of the cells of origin for the various types of HNSCCs probably has some influence on the phenotypes of the malignant cells as well as on host–tumor relationships. Hypopharyngeal carcinomas can nearly be seen as orphan tumors in comparison with other HNSCCs as they are less often the subject of biological investigations.[32] However, it is clear that they have specific clinical and biological characteristics. They are usually more aggressive than HNSCCs at other primary sites, with the highest incidence of distant metastases at the initial stage (60%).[47] Genetic alterations driving their oncogenesis are also distinct with a higher frequency of 11q13 amplifications with predominant involvement of the *FGF3* and *FGF4* genes.[48] There is also preliminary evidence that they have specific features with regard to invasion mechanisms with consistently high expression of MMP2 (matrix metalloproteinase-2 or 72kd type IV collagenase).[49] Our present data suggest that the development of hypopharyngeal carcinomas also relies on distinct mechanisms of tumor suppression with a greater involvement of gal-9 and Kyn than for HNSCCs derived from other primary sites.

To get some clues on whether the excess of plasma gal-9 and kynurenin resulted from their overproduction by tumor cells (either malignant or stromal cells) we resorted to *in silico* analysis, using online bulk RNAseq data from a cohort of 522 HNSCC primary tumor biopsies (Firehose Legacy HNSCC cohort from the TCGA accessed by C-BioPortal). The match was not perfect between gal-9 and Kyn plasma assays in our series and the distribution of gal-9 and IDO1 mRNAs in the various categories of TCGA tumors. While plasma gal-9 and kynurenin were at their highest concentrations for patients with hypopharyngeal carcinomas, gal-9 and IDO1 mRNA expression was maximal in HPV^+ oropharyngeal carcinomas. There are at least three possible explanations for this apparent inconsistency. First, the patients in our cohort were treated for local or metastatic recurrences, which might have biological characteristics distinct from primary tumors. Next, the amounts of gal-9 and IDO1 might be discordant at the mRNA and protein levels. Finally, plasma gal-9 and kynurenin might not be produced solely in the tumor microenvironment. For example, Myeloid-Derived Suppressor Cells (MDSCs) might contribute to their production at the systemic level. Indeed, MDSCs usually have a strong expression of IDO1, while their expansion and maturation are known to be enhanced by extra-cellular gal-9.[41,50,51] These remarks illustrate the need to consider future studies dealing with HNSCC tumors, especially hypopharyngeal carcinomas, and combining plasma assays for gal-9 and Kyn with detection of gal-9 and IDO1 proteins by immunohistochemistry (IHC) in tumor sections. Interestingly, our investigations of TCGA data suggest a positive correlation between gal-9 and IDO1 mRNA expressions in the overall series of HNSCCs and their negative correlation with HIF1α expression. With this in mind, it would be useful to combine IHC for HIF1α with IHC for gal-9 and IDO1 on tumor sections of HNSCCs, especially hypopharyngeal tumors. This type of study might lead us to characterize a potential subset of HNSCCs with a gal-9 high/IDO1 high and HIF1α low pattern. This could have implications for prognosis assessment and therapeutic indications.

Disclosure statement

PB and MD are members of a collaborative project on monoclonal antibodies neutralizing extra-cellular gal-9. This project involves P. Busson's team and HiFIBiO-Therapeutics. Otherwise, the authors declare no potential conflicts of interest.

Funding

This work was supported by the Groupement des Entreprises Françaises dans la Lutte contre le Cancer [2021–2022]; Bristol-Mayer-Squibbs Foundation for Research on Immuno-Oncology [1709-04-040]; Ministère de l'Enseignement Supérieur, de la Recherche et de l'Innovation.

ORCID

Bao-Tram Thi Tran http://orcid.org/0000-0001-7954-696X
Sylvère Durand http://orcid.org/0000-0001-6356-1006
Clémence Toullec http://orcid.org/0000-0003-1733-6945
Karim Benihoud http://orcid.org/0000-0002-9672-5019
Catherine Brenner http://orcid.org/0000-0002-7715-0934
Christophe Le Tourneau http://orcid.org/0000-0001-9772-4686
Toshiro Niki http://orcid.org/0000-0003-4531-1331
Muriel David http://orcid.org/0000-0003-1392-2701
Pierre Busson http://orcid.org/0000-0003-1027-3400

Data availability statements

All data supporting the findings of this study are included in this article or its supplementary material files. Further enquiries can be addressed to the corresponding author.

Authors'contribution

Conception and design of the project: CE, PB, TN, CB, IB and PG. Generation and acquisition of data: BTTT, AG, SD and TN. Analysis and interpretation of the data: BTTT, AG, PB, TN, SD, MD and KB. Statistical analysis: MT with the support of FG. Writing, reviewing and editing were performed by PB with inputs from KB, MD, CE, CLT, JF, AD, CT and CB.

References

1. Bhat GR, Hyole RG, Li J. Head and neck cancer: current challenges and future perspectives. Adv Cancer Res. 2021;152:67–102.
2. Leemans CR, Braakhuis BJ, Brakenhoff RH. The molecular biology of head and neck cancer. Nat Rev Cancer. 2011;11(1):9–22. doi:10.1038/nrc2982.
3. Näsman A, Du J, Dalianis T. A global epidemic increase of an HPV-induced tonsil and tongue base cancer - potential benefit from a pan-gender use of HPV vaccine. J Intern Med. 2020;287(2):134–152. doi:10.1111/joim.13010.
4. Borel C, Jung AC, Burgy M. Immunotherapy breakthroughs in the treatment of recurrent or metastatic head and neck squamous cell carcinoma. Cancers (Basel). 2020;12(9):2691. doi:10.3390/cancers12092691.
5. Burtness B, Harrington KJ, Greil R, Soulières D, Tahara M, de Castro G Jr., Psyrri A, Basté N, Neupane P, Bratland Å, et al. Pembrolizumab alone or with chemotherapy versus cetuximab with chemotherapy for recurrent or metastatic squamous cell carcinoma of the head and neck (KEYNOTE-048): a randomised, open-label, phase 3 study. Lancet. 2019;394(10212):1915–1928. doi:10.1016/S0140-6736(19)32591-7.
6. Clarke E, Eriksen JG, Barrett S. The effects of PD-1/PD-L1 checkpoint inhibitors on recurrent/metastatic head and neck squamous cell carcinoma: a critical review of the literature and meta-analysis. Acta Oncol. 2021;60(1):1–9. doi:10.1080/0284186X.2020.1867766.
7. Botticelli A, Zizzari IG, Scagnoli S, Pomati G, Strigari L, Cirillo A, Cerbelli B, Di Filippo A, Napoletano C, Scirocchi F, et al. The role of soluble LAG3 and soluble immune checkpoints profile in advanced head and neck cancer: a pilot study. J Pers Med. 2021;11(7):651. doi:10.3390/jpm11070651.
8. Kluckova K, Durmanova V, Bucova M. Soluble HLA-G, its diagnostic and prognostic value and potential target molecule for future therapy in cancer. Bratisl Lek Listy. 2021;122(9):60–617. doi:10.4149/BLL_2021_097.
9. Koyama S, Akbay EA, Li YY, Herter-Sprie GS, Buczkowski KA, Richards WG, Gandhi L, Redig AJ, Rodig SJ, Asahina H, et al. Adaptive resistance to therapeutic PD-1 blockade is associated with upregulation of alternative immune checkpoints. Nat Commun. 2016;7(1):10501. doi:10.1038/ncomms10501.
10. Limagne E, Richard C, Thibaudin M, Fumet JD, Truntzer C, Lagrange A, Favier L, Coudert B, Ghiringhelli F. Tim-3/galectin-9 pathway and mMDSC control primary and secondary resistances to PD-1 blockade in lung cancer patients. Oncoimmunology. 2019;8(4):e1564505. doi:10.1080/2162402X.2018.1564505.
11. Navarro P, Martínez-Bosch N, Blidner AG, Rabinovich GA. Impact of galectins in resistance to anticancer therapies. Clin Cancer Res. 2020;26(23):6086–6101. doi:10.1158/1078-0432.CCR-18-3870.
12. Johannes L, Jacob R, Leffler H. Galectins at a glance. J Cell Sci. 2018;131(9). doi:10.1242/jcs.208884.
13. Popa SJ, Stewart SE, Moreau K. Unconventional secretion of annexins and galectins. Semin Cell Dev Biol. 2018;83:42–50. doi:10.1016/j.semcdb.2018.02.022.
14. Chou FC, Chen HY, Kuo CC, Sytwu HK. Role of galectins in tumors and in clinical immunotherapy. Int J Mol Sci. 2018;19(2):430. doi:10.3390/ijms19020430.
15. Gordon-Alonso M, Hirsch T, Wildmann C, van der Bruggen P. Galectin-3 captures interferon-gamma in the tumor matrix reducing chemokine gradient production and T-cell tumor infiltration. Nat Commun. 2017;8(1):793. doi:10.1038/s41467-017-00925-6.
16. Klibi J, Niki T, Riedel A, Pioche-Durieu C, Souquere S, Rubinstein E, Le Moulec S, Guigay J, Hirashima M, Guemira F. Blood diffusion and Th1-suppressive effects of galectin-9–containing exosomes released by Epstein-Barr virus–infected nasopharyngeal carcinoma cells. Blood. 2009;113(9):1957–1966. doi:10.1182/blood-2008-02-142596.
17. Nambiar DK, Aguilera T, Cao H, Kwok S, Kong C, Bloomstein J, Wang Z, Rangan VS, Jiang D, von Eyben R, et al. Galectin-1-driven T cell exclusion in the tumor endothelium promotes immunotherapy resistance. J Clin Invest. 2019;129(12):5553–5567. doi:10.1172/JCI129025.
18. Saussez S, Lorfevre F, Lequeux T, Laurent G, Chantrain G, Vertongen F, Toubeau G, Decaestecker C, Kiss R. The determination of the levels of circulating galectin-1 and −3 in HNSCC patients could be used to monitor tumor progression and/or responses to therapy. Oral Oncol. 2008;44(1):86–93. doi:10.1016/j.oraloncology.2006.12.014.
19. de Oliveira JT, Ribeiro C, Barros R, Gomes C, de Matos AJ, Reis CA, Rutteman GR, Gärtner F. Hypoxia up-regulates galectin-3 in mammary tumor progression and metastasis. PLoS One. 2015;10(7):e0134458. doi:10.1371/journal.pone.0134458.
20. Gu X, Meng H, Wang J, Wang R, Cao M, Liu S, Chen H, Xu Y. Hypoxia contributes to galectin-3 expression in renal carcinoma cells. Eur J Pharmacol. 2021;890:173637. doi:10.1016/j.ejphar.2020.173637.
21. Wang L, Li YS, Yu LG, Zhang XK, Zhao L, Gong FL, Yang XX, Guo XL. Galectin-3 expression and secretion by tumor-associated macrophages in hypoxia promotes breast cancer progression. Biochem Pharmacol. 2020;178:114113. doi:10.1016/j.bcp.2020.114113.
22. Darrow AL, Shohet RV. Galectin-3 deficiency exacerbates hyperglycemia and the endothelial response to diabetes. Cardiovasc Diabetol. 2015;14(1):73. doi:10.1186/s12933-015-0230-3.
23. Chang H, Xu Q, Li J, Li M, Zhang Z, Ma H, Yang X. Lactate secreted by PKM2 upregulation promotes Galectin-9-mediated immunosuppression via inhibiting NF-κB pathway in HNSCC. Cell Death Dis. 2021;12(8):725. doi:10.1038/s41419-021-03990-4.
24. Duchemann B, Remon J, Naigeon M, Mezquita L, Ferrara R, Cassard L, Jouniaux JM, Boselli L, Grivel J, Auclin E, et al. Integrating circulating biomarkers in the immune checkpoint inhibitor treatment in lung cancer. Cancers (Basel). 2020;12(12):3625.
25. Bellutti Enders F, van Wijk F, Scholman R, Hofer M, Prakken BJ, van Royen-Kerkhof A, de Jager W. Correlation of CXCL10, tumor necrosis factor receptor type II, and galectin 9 with disease activity in juvenile dermatomyositis. Arthritis Rheumatol. 2014;66(8):2281–2289. doi:10.1002/art.38676.
26. Martinez-Bosch N, Barranco LE, Orozco CA, Moreno M, Visa L, Iglesias M, Oldfield L, Neoptolemos JP, Greenhalf W, Earl J, et al. Increased plasma levels of galectin-1 in pancreatic cancer: potential use as biomarker. Oncotarget. 2018;9(68):32984–32996. doi:10.18632/oncotarget.26034.
27. Yogasundaram H, Nikhanj A, Putko BN, Boutin M, Jain-Ghai S, Khan A, Auray-Blais C, West ML, Oudit GY. Elevated inflammatory plasma biomarkers in patients with Fabry disease: a critical link to heart failure with preserved ejection fraction. J Am Heart Assoc. 2018;7(21):e009098. doi:10.1161/JAHA.118.009098.
28. Zhao CN, Mao YM, Liu LN, Wu Q, Dan YL, Pan HF. Plasma galectin-3 levels do not differ in systemic lupus erythematosus patients. Int J Rheum Dis. 2019;22(10):1820–1824. doi:10.1111/1756-185X.13677.
29. Tsugawa H, Tsujimoto Y, Sugitate K, Sakui N, Nishiumi S, Bamba T, Fukusaki E. Highly sensitive and selective analysis of widely targeted metabolomics using gas chromatography/triple--quadrupole mass spectrometry. J Biosci Bioeng. 2014;117(1):122–128. doi:10.1016/j.jbiosc.2013.06.009.
30. Viltard M, Durand S, Pérez-Lanzón M, Aprahamian F, Lefevre D, Leroy C, Madeo F, Kroemer G, Friedlander G. The metabolomic signature of extreme longevity: naked mole rats versus mice. Aging (Albany NY). 2019;11(14):4783–4800. doi:10.18632/aging.102116.

31. «World Medical Association Declaration of Helsinki: Ethical Principles for Medical Research Involving Human Subjects». JAMA. 2013;310:2191–2194. DOI:10.1001/jama.2013.281053
32. Garneau JC, Bakst RL, Miles BA. Hypopharyngeal cancer: a state of the art review. Oral Oncol. 2018;86:244–250. doi:10.1016/j.oraloncology.2018.09.025.
33. Mito I, Takahashi H, Kawabata-Iwakawa R, Ida S, Tada H, Chikamatsu K. Comprehensive analysis of immune cell enrichment in the tumor microenvironment of head and neck squamous cell carcinoma. Sci Rep. 2021;11(1):16134. doi:10.1038/s41598-021-95718-9.
34. Anderson AC, Anderson DE, Bregoli L, Hastings WD, Kassam N, Lei C, Chandwaskar R, Karman J, Su EW, Hirashima M, et al. Promotion of tissue inflammation by the immune receptor Tim-3 expressed on innate immune cells. Science. 2007;318(5853):1141–1143. doi:10.1126/science.1148536.
35. Henderson NC, Sethi T. The regulation of inflammation by galectin-3. Immunol Rev. 2009;230(1):160–171. doi:10.1111/j.1600-065X.2009.00794.x.
36. Sundblad V, Morosi LG, Geffner JR, Rabinovich GA. Galectin-1: a Jack-of-All-Trades in the resolution of acute and Chronic inflammation. J Immunol. 2017;199(11):3721–3730. doi:10.4049/jimmunol.1701172.
37. Valdes M, Villeda J, Mithoowani H, Pitre T, Chasen M. Inflammatory markers as prognostic factors of recurrence in advanced-stage squamous cell carcinoma of the head and neck. Curr Oncol. 2020;27(3):135–141. doi:10.3747/co.27.5731.
38. De Benedetti F, Prencipe G, Bracaglia C, Marasco E, Grom AA. Targeting interferon-γ in hyperinflammation: opportunities and challenges. Nat Rev Rheumatol. 2021;17(11):678–691. doi:10.1038/s41584-021-00694-z.
39. Beasley NJ, Leek R, Alam M, Turley H, Cox GJ, Gatter K, Millard P, Fuggle S, Harris AL. Hypoxia-inducible factors HIF-1alpha and HIF-2alpha in head and neck cancer: relationship to tumor biology and treatment outcome in surgically resected patients. Cancer Res. 2002;62:2493–2497.
40. Coppock JD, Mills AM, Stelow EB. Galectin-3 expression in high-Risk HPV-positive and negative head & neck squamous cell carcinomas and regional lymph node metastases. Head Neck Pathol. 2021;15(1):163–168. doi:10.1007/s12105-020-01195-3.
41. Zhai L, Ladomersky E, Lenzen A, Nguyen B, Patel R, Lauing KL, Wu M, Wainwright DA. IDO1 in cancer: a Gemini of immune checkpoints. Cell Mol Immunol. 2018;15(5):447–457. doi:10.1038/cmi.2017.143.
42. Castro-Portuguez R, Sutphin GL. Kynurenine pathway, NAD(+) synthesis, and mitochondrial function: targeting tryptophan metabolism to promote longevity and healthspan. Exp Gerontol. 2020;132:110841. doi:10.1016/j.exger.2020.110841.
43. Mezrich JD, Fechner JH, Zhang X, Johnson BP, Burlingham WJ, Bradfield CA. An interaction between kynurenine and the aryl hydrocarbon receptor can generate regulatory T cells. J Immunol. 2010;185(6):3190–3198. doi:10.4049/jimmunol.0903670.
44. Campesato LF, Budhu S, Tchaicha J, Weng CH, Gigoux M, Cohen IJ, Redmond D, Mangarin L, Pourpe S, Liu C, et al. Blockade of the AHR restricts a Treg-macrophage suppressive axis induced by L-Kynurenine. Nat Commun. 2020;11(1):4011. doi:10.1038/s41467-020-17750-z.
45. Bishnupuri KS, Alvarado DM, Khouri AN, Shabsovich M, Chen B, Dieckgraefe BK, Ciorba MA. IDO1 and kynurenine pathway metabolites activate PI3K-Akt signaling in the neoplastic colon epithelium to promote cancer cell proliferation and inhibit apoptosis. Cancer Res. 2019;79(6):1138–1150. doi:10.1158/0008-5472.CAN-18-0668.
46. Cillo AR, Kürten CHL, Tabib T, Qi Z, Onkar S, Wang T, Liu A, Duvvuri U, Kim S, Soose RJ, et al. Immune landscape of viral- and carcinogen-driven head and neck cancer. Immunity. 2020;52(1):183–199.e189. doi:10.1016/j.immuni.2019.11.014.
47. Kotwall C, Sako K, Razack MS, Rao U, Bakamjian V, Shedd DP. Metastatic patterns in squamous cell cancer of the head and neck. Am J Surg. 1987;154(4):439–442. doi:10.1016/0002-9610(89)90020-2.
48. Rodrigo JP, Suárez C, González MV, Lazo PS, Ramos S, Coto E, Alvarez I, García LA, Martínez JA. Variability of genetic alterations in different sites of head and neck cancer. Laryngoscope. 2001;111(7):1297–1301. doi:10.1097/00005537-200107000-00029.
49. Répássy G, Forster-Horváth C, Juhász A, Adány R, Tamássy A, Tímár J. Expression of invasion markers CD44v6/v3, NM23 and MMP2 in laryngeal and hypopharyngeal carcinoma. Pathol Oncol Res. 1998;4(1):14–21. doi:10.1007/BF02904689.
50. Dardalhon V, Anderson AC, Karman J, Apetoh L, Chandwaskar R, Lee DH, Cornejo M, Nishi N, Yamauchi A, Quintana FJ, et al. Tim-3/galectin-9 pathway: regulation of Th1 immunity through promotion of CD11b+Ly-6G+ myeloid cells. J Immun. 2010;185(3):1383–1392. doi:10.4049/jimmunol.0903275.
51. Zhang CX, Huang DJ, Baloche V, Zhang L, Xu JX, Li BW, Zhao XR, He J, Mai HQ, Chen QY, et al. Galectin-9 promotes a suppressive microenvironment in human cancer by enhancing STING degradation. Oncogenesis. 2020;9(7):65. doi:10.1038/s41389-020-00248-0.